Proceedings of Ninth World Conference on Earthquake Engineering
August 2-9, 1988, Tokyo-Kyoto, JAPAN (Vol.VIII)

SL-1

STRENGTH OF EARTHEN WALL SUBASSEMBLIES: AN EXPERIMENTAL AND ANALYTICAL STUDY

Polat Gülkan[1] and Fikret Gürdil[2]

1 Basler & Hofmann, Consulting Engineers, 8029 Zürich, Switzerland; on leave from Department of Nuclear Energy Engineering, Hacettepe University, 06532 Beytepe, Ankara, Turkey
2 Temelsu Engineering Inc., Cankaya, Ankara, Turkey

SUMMARY

An experimental study of the strength of square adobe walls subjected to constant in-plane compression normal to the horizontal mortar joints and an incrementally applied diagonal load is described. Within the range of the loads considered in the experimental phase an increase in the diagonal load carrying capacity was observed in the specimens. The biaxial strength of the assemblies could be satisfactorily computed in a qualitative way by an incremental nonlinear finite element analysis when the soil was represented as an elastic-plastic material obeying the Mohr-Coulomb failure criterion.

INTRODUCTION

Earthen dwellings provide shelter to people in many diverse parts of the world. Their notoriously low resistance against earthquake effects makes this class of structures very hazardous because of the loss of lives their collapse has been known to cause. The modes of failure in adobe houses have been identified, but varying and often unstandardized construction techniques, vernacular forms and the inherent randomness of the properties of the constituents have impeded a better understanding of the behavior of earthen (or, in a narrower sense, adobe) buildings in mechanistic terms.

The objective of the research reported here has been to investigate experimentally the strength of square adobe wall specimens subjected simultaneously to in-plane compressive and shear forces similar to the way in which walls would be stressed in a house subjected to an earthquake. This phase involved parallel experiments to establish the physical properties of the ingredients, (Ref. 1). In the following analytical phase correlations were made between the experiments and theoretical predictions of capacity incorporating plasticity theory.

EXPERIMENTAL PROGRAM

Test Specimens and Arrangement. Within limitations dictated by the available facilities the easiest way of determining the capacity of the walls loaded as described earlier was the arrangement in Fig. 1. The specimens measured nominally 1x1x0.3 m, and care was taken to reduce the effects of stress concentrations near the diagonally opposite load fixtures. All of the wall units and the the bricks used in making them were prepared by experienced journeyman masons.

Material Properties. The strength and mechanical properties of the walls were determined from tests on prisms and assemblies made together with the walls. The soil properties are listed in Table 1. The water/soil weight ratio was 0.41 for the adobe bricks which contained also 1 percent straw to reduce the effect of shrinkage. The full-size units measured 0.4x0.3x0.12 m, the half units 0.18x 0.3x0.12 m. In Table 2 we list the properties of the bricks and the prisms.

The tensile strength of 588 kPa in Table 2 was determined from specially made briquettes with an area of 500 mm2 (Ref. 2). This is very high, especially in comparison with modulus of rupture values ranging between 40-350 kPa, and the compressive strength of the prisms. One reason may be the high clay content of the soil, and another the lack of shrinkage cracks in the samples.

Conduct of Experiments. Small wedges were cut from the two diagonally opposite corners of the walls to apply the diagonal load P_d. The vertical load P_v was applied by a testing machine through a system which minimized friction against displacements in the upper edge. In- and out-of-plane displacements and forces were monitored during the experiments which included 5 walls.

Review of the Experiments. A summary is provided for the measurements in Table 3. Here, b t = product of the measured cross section dimensions of wall area, P_v= (constant) edge load, $(P_d)_{max}$= maximum diagonal load, $-\sigma_v = P_v/b\,t$, $-\sigma_y' = (P_v + 0.707(P_d)_{max})/b\,t$, $\tau_d' = 0.707\,(P_d)_{max}/b\,t$. We denote the value of τ_d' in the absence of edge load as $\tilde{\tau}_d'$, and normalize the total normal stress and shear stress with respect to this value in the last two columns. The value $\tilde{\tau}_d' = 71.5$ kPa was determined from a regression analysis on data from Walls 1-4. Wall 5 was tested under an edge stress greater than half of the average compressive strength of the wall prisms. The diagonal failure load for this wall suggests that its actual strength may have been atypical.

Discussion of the Experiments. It is instructive to write the expressions for the principal stresses in the middle of a wall loaded as in Fig. 1, (Ref. 3):

$$\sigma_{1,3} = -0.823\,\tau_d' + \sigma_v/2 \pm \sqrt{(1.556\,\tau_d')^2 + \sigma_v^2/4} \qquad (1)$$

The limiting cases of no edge load and no diagonal load can be checked from Eq. (1), and the corresponding directions of the principal stresses found. For the plane stress condition of the experiments the intermediate principal stress is zero. The tests showed that the edge stress affected the strength of the walls significantly. Within the range of the applied edge stresses the diagonal capacity increased with larger edge surcharge. When larger edge stresses were applied the direction of the minor principal axis, as inferred from the cracks, rotated towards the normal to the horizontal joint resulting in splitting failures at the center of the panels rather than joint separation typical of small edge stresses. Walls 1 and 2 behaved in this way: with increasing P_d cracks propagated along the mortar joints and culminated in a mechanism of slippage where cracks developed into a staggered path. In Wall 3 diagonal load-deformation was linear until the total edge stress reached 245 kPa. At 300 kPa cracks in the loaded diagonal direction appeared, and intersected the units. Increased diagonal load caused splitting in the blocks at the center, but failure occurred when units near the load fixtures failed. Splitting of the blocks by a crack originating near the center was clearer in Wall 4. The failure pattern for Wall 5 was interesting because in combination with the diagonal cracks arising from the splitting of the blocks, vertical cracks also developed and it failed when the central part was crushed.

In summary, the experiments showed that the relation between the shear and compressive strength in the range $1 < R = -\sigma'_y/\tilde{\tau}'_d < 4$ or 5 was linear, and failure was by joint separation. In the range $5 < R < 7$ failure appeared to be joint separation combined with splitting of the units along the loaded diagonal. Beyond $R > 7$ failure was primarily by splitting or crushing.

FAILURE ANALYSIS

A progressive analysis to failure of the wall in Fig. 1 requires consideration of the manner in which the loads are applied to it, behavior of the material in general terms and an analytical procedure with a statement of what is implied by its failure, (Ref. 4). In the computational phase the objective was determined as one of duplicating the overall strength characteristics of adobe walls rather than mimicking the measured behavior of the walls which would have been a fruitless exercise because of the large number of tests required for a meaningful set of results. Here, the adobe and mortar were assumed to be linearly elastic-perfectly plastic (nonhardening) isotropic brittle materials. The constitutive law adopted for both ingredients was the Mohr-Coulomb model for which the failure envelope is defined with the expression

$$|\tau| = c - \sigma \tan\phi \tag{2}$$

In terms of the principal stresses the failure condition in Eq.(2) is:

$$\sigma_1 \frac{(1 - \sin\phi)}{2\ c\ \cos\phi} - \sigma_3 \frac{(1 + \sin\phi)}{2\ c\ \cos\phi} = 1 \tag{3}$$

The shape of the failure criterion in two-dimensional stress space is the irregular hexagon in Fig. 2.

In terms of the uniaxial compressive strength f'_{ca} and tensile strength f'_{ta} the material constants c and ϕ are

$$c = 0.5 \sqrt{f'_{ca}\ f'_{ta}} \tag{4}$$

$$\phi = \sin^{-1} \frac{f'_{ca} - f'_{ta}}{f'_{ca} + f'_{ta}} \tag{5}$$

The analysis for the 1 m square walls was made for two values of the tensile strength for the adobe units: 588 kPa to reflect the briquette tests, and 120 kPa, typical of modulus of rupture tests; f'_{ca} was constant at 1100 kPa.

Nonlinear quadrilateral isoparametric plane elements were used, (Ref. 5). In contrast to the physical tests the model was rotated by 45 degrees for a better representation of the idealized boundary conditions. The edge pressure was brought up to the desired value in increments before the diagonal load was applied, also incrementally, until no further increase could be achieved or numerical instabilities violated the prescribed tolerances.

Discussion of the Results. The computed strength envelopes are shown in Fig. 3. The axes have been normalized as in Table 3, and the experimental results given alongside the computed curves. The larger f'_{ta} predicts only a modest 20 percent increase in the nominal shear strength while the smaller value of 120 kPa leads to a two-fold increase in the region $-\sigma'_y/\tilde{\tau}'_d = 4$ to 5, and the diagonal com-

pressive strength under edge load is not less than that under no edge load until $-\sigma'_y/\tilde{\tau}'_d > 8$. The two curves intersect the horizontal axis at values differing by nearly a factor of 2 because of the way they have been normalized. The distorted geometries in Fig. 4 give indirect clues to the failure mechanism:at very small or very large edge stresses the failure occurs with no redistribution of stresses, while edge stresses in the range 200-600 kPa cause an effectively more ductile assembly. In Fig. 4 a constant value has been assigned to the largest displacement in the deformed mesh; in Fig. 5 we show the actual indicative values. The brittle response at no edge stress is similar to that under an edge stress only 9 percent smaller than f'_{ca}.

It is useful to study the variation of the "pure" diagonal compressive strength, $\tilde{\tau}'_d$, when only the uniaxial tensile strength is allowed to vary, with $\sigma_v = 0$. With $f'_{ca} = 1100$ kPa a series of $(P_d)_{max}$ were computed for $f'_{ta} = 80$, 200, and 400 kPa in addition to the values 120 and 588 kPa. As Fig. 6 indicates, the maximum diagonal load is very strongly dependent on the tensile strength as long as it is less than about 1/4 of the compressive strength. For larger f'_{ta}/f'_{ca} ratios it is the compressive strength which governs $(P_d)_{max}$. This is also hidden in Eq. (1): solving for the principal stresses at the center of the panel when $\sigma_v = 0$, one determines $\sigma_{1,3} = 0.734\ \tilde{\tau}'_d$, $-2.380\ \tilde{\tau}'_d$. The ratio of these is 0.3, so it is only when f'_{ta}/f'_{ca} is less than this value that the diagonal load at failure can have any dependence on tensile strength. The conclusion which immediately follows from this observation is that in the test walls the actual effective tensile strength must have been smaller than 120 kPa. When a smaller $\tilde{\tau}'_d$ is used in normalizing the axes in Fig. 3, a better agreement is achieved.

CONCLUSIONS

1. Failure under compressive edge and diagonal loads in adobe walls was due to joint separation at small edge loads ($-\sigma'_y/\tilde{\tau}'_d < 4$) and crushing or splitting at large edge loads ($-\sigma'_y/\tilde{\tau}'_d > 8$). A transition occurred in between.

2. It was possible to capture the characteristics of the overall behavior of the walls tested in terms of strength through a computational procedure where the failure law for adobe walls was expressed with the Mohr-Coulomb criterion. Proper assessment of the strength parameters brings a better reconciliation between the test results and the subsequent calculations.

ACKNOWLEDGMENTS

The tests described in the text were conducted under a project funded by the Earthquake Research Division of the Turkish Ministry of Public Works and Housing. Basler & Hofmann, Consulting Engineers, Zürich made available extensive facilities for the computational part of the investigation. Thanks are due also for the fruitful discussions with P. Bartelt of the Swiss Federal Institute of Technology, Zürich, Institute of Informatics.

REFERENCES

1. Gürdil, F., "An Investigation of the Failure Criteria for Adobe Walls," Ph.D. dissertation, Department of Civil Engineering, Middle East Technical University, Ankara, Turkey, (1986).

2. American Society for Testing and Materials, "Test for Tensile Strength of Hydraulic Cement Mortars," ASTM-C190, (1972).
3. Yokel, F.Y., and S.G. Fattal, "Failure Hypothesis for Masonry Shear Walls," Journal of the Structural Division, ASCE, Vol. 102, No.ST3, March, (1976).
4. Chen, W.F., and A.F. Saleeb, Constitutive Equations for Engineering Materials, Wiley, (1982).
5. Anderheggen, E., et al., "FLOWERS Users Manual," Swiss Federal Institute of Technology, Zürich, Institute of Informatics, Third Ed., (1985).

TABLE 1. Adobe Soil Properties

Dry unit weight, kN/m3	16 300	Shrinkage limit, %	13.3
Specific gravity	2.68	Plastic limit, %	16.3
Natural water content, %	34	Liquid limit, %	47.1
Normal consistency, %	18.1	Clay content, %	31
Optimum water content, %	21	1-day tensile strength, kPa	45
Shrinkage, %	7	7-day comp. strength, kPa	2880
		28-day comp. strength, kPa	3810

TABLE 2. Properties of Adobe Bricks and Assemblies

Type of Test	Unit	Age (Days)	Average Test Result	Number of Units	Coefficient of Variation (Percent)
Tensile strength	Special Briquette	7	206 kPa	6	19.3
		28	588 kPa	6	11.9
Compressive strength	Pair of 1/2 units	28	1167 kPa	5	7.2
Compressive strength	Single 1/2 units	28	1638 kPa	2	-
		360	4433 kPa	5	4.8
Compressive strength	Single full unit	360	4068 kPa	5	1.4
Compressive strength	0.96 m prism	371	1080 kPa	3	19
Elastic modulus	Single 1/2 unit	28	46 MPa	2	-
		360	79 MPa	5	13
Elastic modulus	Single full unit	360	107 MPa	5	2

TABLE 3. Test Results

Specimen	b t m2	P_v kN	$(P_d)_{max}$ kN	$-\sigma_v$ kPa	$-\sigma_y'$ kPa	τ_d' kPa	$-\sigma_y'/\tilde{\tau}_d'$	$\tau_d'/\tilde{\tau}_d'$
Wall 1	0.2435	19.32	43.61	79.4	206.0	126.6	2.88	1.77
Wall 2	0.2469	24.62	54.92	99.7	257.0	157.3	3.59	2.20
Wall 3	0.2482	46.33	77.15	186.7	406.5	219.8	5.69	3.07
Wall 4	0.2375	69.33	100.68	291.9	591.7	299.8	8.28	4.19
Wall 5	0.2372	158.93	185.67	670.0	1223.5	553.5	17.11	7.74

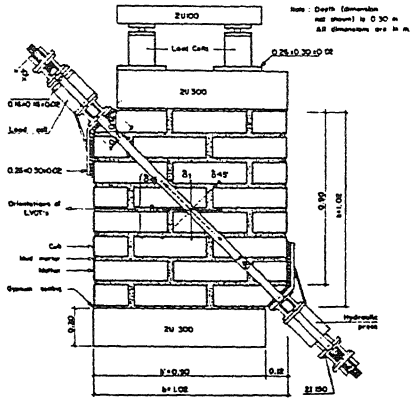

Fig. 1 Experimental Setup and Test Wall

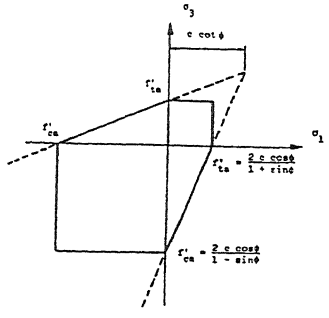

Fig. 2 Mohr-Coulomb Criterion

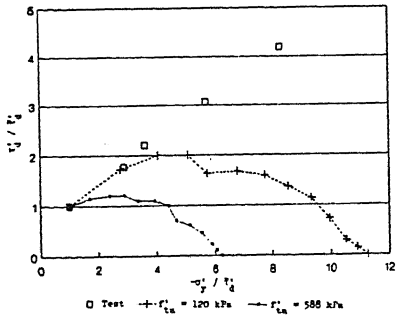

Fig. 3 Comparison of Results

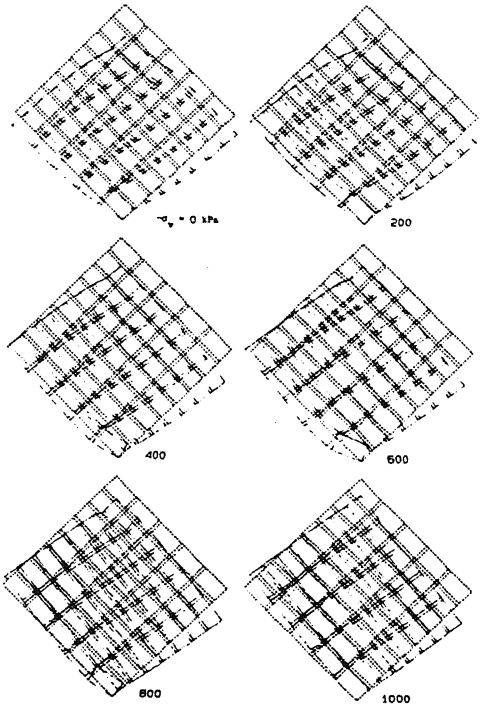

Fig. 4 Computed Deformed Shapes at Failure

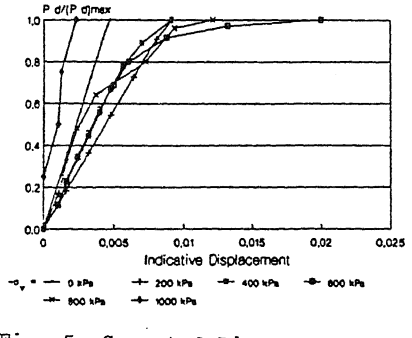

Fig. 5 Computed Displacement along Loaded Diagonal

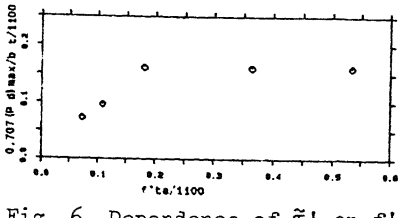

Fig. 6 Dependence of $\tilde{\tau}'_d$ on f'_{ta}